

Physiological Gain Leads to High ISI Variability in a Simple Model of a Cortical Regular Spiking Cell

Todd W. Troyer

*Keck Center for Integrative Neuroscience, Department of Physiology,
University of California, San Francisco, San Francisco, CA 94143 USA*

Kenneth D. Miller

*Keck Center for Integrative Neuroscience and Sloan Center for Theoretical Neurobiology,
Departments of Physiology and Otolaryngology, University of California,
San Francisco, San Francisco, CA 94143 USA*

To understand the interspike interval (ISI) variability displayed by visual cortical neurons (Softky & Koch, 1993), it is critical to examine the dynamics of their neuronal integration, as well as the variability in their synaptic input current. Most previous models have focused on the latter factor. We match a simple integrate-and-fire model to the experimentally measured integrative properties of cortical regular spiking cells (McCormick, Connors, Lighthall, & Prince, 1985). After setting RC parameters, the post-spike voltage reset is set to match experimental measurements of neuronal gain (obtained from *in vitro* plots of firing frequency versus injected current). Examination of the resulting model leads to an intuitive picture of neuronal integration that unifies the seemingly contradictory $1/\sqrt{N}$ and random walk pictures that have previously been proposed. When ISIs are dominated by postspike recovery, $1/\sqrt{N}$ arguments hold and spiking is regular; after the “memory” of the last spike becomes negligible, spike threshold crossing is caused by input variance around a steady state and spiking is Poisson. In integrate-and-fire neurons matched to cortical cell physiology, steady-state behavior is predominant, and ISIs are highly variable at all physiological firing rates and for a wide range of inhibitory and excitatory inputs.

1 Introduction ---

Softky and Koch (1993) have shown that the spike trains of cortical cells in visual areas V1 and MT display a high degree of variability, as measured by their interspike interval (ISI) distributions at fixed mean firing rates. Does this result require revising the classical notion of information transmission in cortical neurons? By “classical notion,” we mean the view that neurons integrate many synaptic inputs until reaching some voltage threshold, and at that point produce a spike. Spikes are then followed by a refractory period,

during which the cell is less likely to produce another spike. If inputs are uncorrelated, the mean spike rate of such a model neuron depends on the average frequency of presynaptic events and thus can embody the standard notion of rate coding.

Softky and Koch (1993) argued that high ISI variability is inconsistent with a neuron's acting as an EPSP integrator. The integration of many uncorrelated excitatory synaptic potentials (EPSPs) should result in a time to threshold (or ISI) that is very regular, since the neuron averages over many random events. One measure of spike variability is the coefficient of variation (CV) of the ISI distribution, defined as the standard deviation divided by the mean. For an EPSP integrator, this should be approximately $1/\sqrt{N}$, where N is the number of events necessary to reach threshold. In contrast, cortical cells have CVs in the range .5 to 1, more closely resembling a random (i.e., Poisson) process for which $CV = 1$. As an alternative to simple integration, Softky and Koch (1993) proposed that active dendritic conductances may act to amplify submillisecond coincidences in synaptic input, leading to large random pulses of synaptic current. Thus, they suggested that high ISI variability may be more consistent with the notion (Abeles, 1982) of neurons acting as "coincidence detectors" rather than "rate encoders."

Shadlen and Newsome (1994), following Gerstein and Mandelbrot (1964), argued that if uncorrelated synaptic inputs to a cell consist of balanced excitation and inhibition, then the membrane voltage follows a random walk, leading to ISIs that are quite variable. This balanced inhibition model is consistent with the classical notion of synaptic integration and rate coding but requires that excitation and inhibition be tightly balanced in order to achieve ISI variability consistent with the data.

These arguments can be more clearly understood by considering spike production as a two-step process. First, synaptic inputs are integrated by an extensive and complex dendritic tree resulting in a total synaptic current $I(t)$. Second, the cell produces spikes in response to this synaptic current. Thus, we expect that spike variability should depend on two factors: the sensitivity of the spike mechanism to changes in the synaptic current and the variability in this input current.

Previous discussions of ISI variability have largely focused on the second term, that is, under what conditions sufficient input variability can be achieved. Thus, Softky and Koch (1993) argued that input current variability was too low to account for output spiking variability, while Shadlen and Newsome (1994) argued that a balance of excitation and inhibition could yield high input variability. Other models demonstrated that network dynamics can lead to correlations among synaptic inputs sufficient to yield high variability (Usher, Stemmler, Koch, & Olami, 1994; Hansel & Sompolinsky, 1996) (afferent inputs also have significant correlations; Alonso, Usrey, & Reid, 1996). However, these investigations generally did not address the sensitivity of cortical neurons. Neuronal sensitivity has been addressed by Bell, Mainen, Tsodyks, and Sejnowski (1995), who considered some of the

same factors as our work in the context of a Hodgkin-Huxley model.¹ Our work differs in considering simple integrate-and-fire dynamics focusing on the roles of gain and refractoriness, and, most important, matching model parameters to experimental data from cortical neurons.

For the purposes of this article, we define neuronal gain as the slope of a plot of firing frequency $f = 1/ISI$ versus the (constant) level of injected current I . Although there is no direct relationship between this measure and neuronal sensitivity under physiological conditions—neuronal gain is measured in the absence of input variability—we will argue that the two should be well correlated. Here we demonstrate that matching a simple integrate-and-fire model to experimentally measured values of neuronal gain can largely solve the conundrum of high ISI variability in visual cortical cells with many random synaptic inputs. A careful examination of this model leads to a relatively simple, intuitive picture of cortical neuronal integration that unifies the seemingly contradictory $1/\sqrt{N}$ and random walk pictures that have been previously proposed.

A preliminary report of this study has appeared as an abstract (Troyer & Miller, 1995).

2 The High-Gain Model

In an integrate-and-fire model, the slower, integrative properties of neurons are modeled as passive changes in subthreshold membrane voltage. The fast spiking conductances are lumped into a stereotyped event that is “pasted onto” the voltage trace when the cell reaches threshold. After spiking, there is an absolute refractory period during which the cell cannot spike, followed by a relative refractory period during which the cell’s ability to spike is reduced. We will use refractoriness to refer to the combined effect of all processes occurring after a spike that make a cell less likely to respond to a given pattern of input current with a subsequent spike. Refractoriness can be defined quantitatively as a function r of the time t after a given spike as follows. Suppose a just-threshold DC current is applied at or before the spike time, $t = 0$. The refractoriness, $r(t)$, is the magnitude of a brief current pulse that, superimposed on this ongoing DC current at time t , is just sufficient to elicit a spike.² Note that this definition includes all factors that contribute to the cell’s refractoriness, including sodium channel inactivation and the ef-

¹ Bell et al. (1995) and Wilbur and Rinzel (1983) also investigated bistability in neuronal dynamics as a mechanism that could contribute to ISI variability.

² Assume a spike occurs at $t = 0$, and that after an absolute refractory period t_{refract} the voltage is reset to V_{reset} . Let τ be the membrane time constant, g_{leak} the leak conductance, and Δt the duration of the brief current pulse. Beginning from V_{reset} at time $t = t_{\text{refract}}$, let I_t be the DC current that leads to a spike at time t' (so I_{∞} is the just-threshold DC current). Let $V_t(t)$ be the time course of the voltage given I_t . Then $r(t) \equiv \frac{I_t}{\Delta t} g_{\text{leak}} (V_t(t) - V_{\infty}(t)) = (I_t - I_{\infty})(1 - e^{-(t-t_{\text{refract}})/\tau}) \frac{I_t}{\Delta t}$.

fects of other active conductances, as well as spike after-hyperpolarization.³ In the simplest models, refractory effects are modeled by waiting for a fixed, absolute refractory period after spike onset and then resetting the voltage to a value significantly below threshold. Thus, a single parameter, the depth of the after-spike voltage reset, serves to model all of the elements contributing to the cell's relative refractoriness.⁴ More realistic models of the complex events following a cortical spike may deepen our understanding of cortical integration, but such models are experimentally poorly constrained and can lose the clarity motivating the use of simple models.

We use a simple conductance-based integrate-and-fire model:

$$C \frac{\partial V}{\partial t} = g_{\text{leak}}(V_{\text{rest}} - V) + I. \quad (2.1)$$

Parameters were matched to slice recordings of regular spiking cells (values from McCormick et al., 1985, noted in parentheses): $V_{\text{rest}} = -74$ (73.6 ± 1.5) mV; $1/g_{\text{leak}} = 40$ (39.9 ± 21.2) $M\Omega$; $C = \tau g_{\text{leak}}$ where $\tau = 20$ (20.2 ± 14.6) msec.⁵ The absolute refractory period was taken to be the spike width, $t_{\text{spike}} = 1.75$ ($1.74 \pm .41$) msec. Spike threshold V_{thresh} was set 20 mV above V_{rest} : $V_{\text{thresh}} = -54$ mV. This leaves the after-spike reset voltage, V_{reset} , as the only free parameter. This parameter is commonly set equal to V_{reset} , but this choice lacks physiological justification.

We set V_{reset} to match the model's f-I curve to that observed physiologically, as reported in McCormick et al. (1985) (see Figure 1A). That is, we set V_{reset} to match the physiologically observed neuronal gain.⁶ This yields $V_{\text{reset}} = -60$ mV, 6 mV below threshold. Using the f-I curve to set V_{reset} points to the strong connection between refractoriness and neuronal gain. Once τ and g_{leak} are determined from biophysical measurements, neuronal gain is determined by the cell's refractory behavior. A cell that is more refractory requires more input current to spike at any given frequency, resulting in an inverse relationship between refractoriness and neuronal

³ After-hyperpolarization—the voltage state of the cell—is often regarded as affecting integration rather than refractoriness, with “refractoriness” reserved for processes that alter the cell's spike responses at a given voltage, such as spike threshold elevation. When considering a cell's reduced responsiveness to input currents, however, it is most useful to combine all factors contributing to the reduction.

⁴ Alternatively, one may consider a two- (or three-) parameter model of refractoriness in which instead of (or in addition to) postspike voltage reset, there is a postspike elevation of threshold that decays at some rate (reviewed in Tuckwell, 1988, Table 3.1).

⁵ The term *regular spiking* denotes the class of cortical cells that respond to constant current injection in vitro with single-spike firing and spike-rate adaptation (McCormick et al., 1985). These constitute most cortical excitatory cells. The term does not imply regularity of firing in vivo.

⁶ Matching the slope of the model f-I curve at 100 Hz to the average gain reported by McCormick et al. (1985) for cortical regular firing cells gives $V_{\text{reset}} = -59.75$ mV.

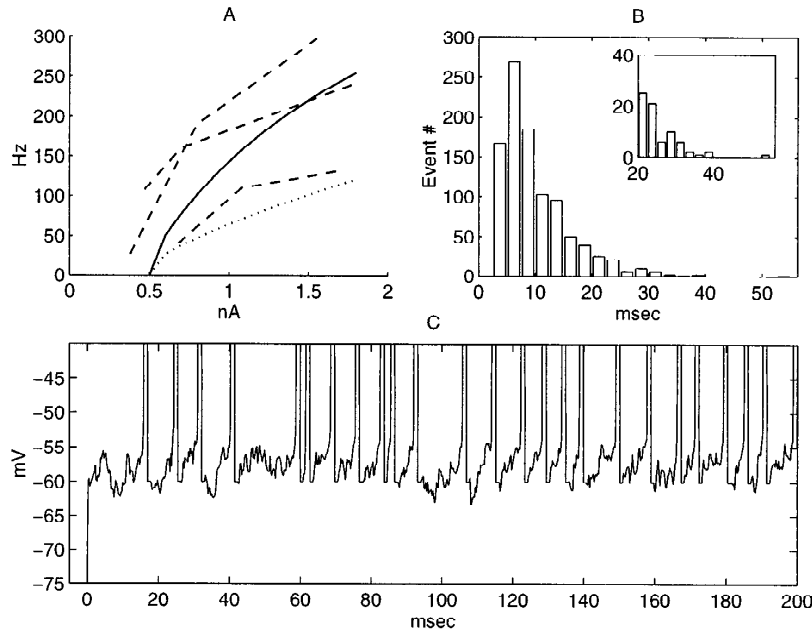


Figure 1: (A) f-I plots for our high-gain model (solid line) and experiment (dashed line). For comparison, the dotted line represents the more common low-gain model, in which V_{reset} is set to V_{rest} . Experimental data shown are piecewise linear fits to data for first interspike interval from three cells (McCormick et al. 1985, Fig. 1). (B) ISI histogram from 10 sec of model data: $\lambda_{\text{ex}} = 7015$ Hz; $\lambda_{\text{in}} = 3263$ Hz ($R = .75$); average firing rate = 98.4 Hz; $CV = .6$. Inset shows ISIs > 20 msec. (C) Voltage trace of first 200 msec of simulation in (B).

gain.⁷ Similarly, greater refractoriness implies weaker sensitivity to physiological inputs. This explains why we connect high gain measured with constant currents to high sensitivity under physiological conditions: For a given membrane time constant and input resistance, weaker refractoriness implies both higher gain and higher physiological sensitivity.

Synaptic input took the form of Poisson distributed delta function conductance changes, $I_{\text{syn}}(t) = \sum_k g_{\text{syn}} \delta(t - t_k) (V_{\text{syn}} - V)$, where t_k denotes the

⁷ Using the definitions of note 2, $r(t) = (I_t - I_{\infty})(1 - e^{-(t-t_{\text{refract}})/\tau}) \frac{\tau}{\Delta t}$. Writing gain $G(f)$ as a function of firing frequency f ($G(f)$ is the slope of the f - I curve at f), this yields $r(t) = (1 - e^{-(t-t_{\text{refract}})/\tau}) \frac{\tau}{\Delta t} \int_{f=0}^{f=1/t} df/G(f)$. Thus, high gain corresponds to low refractoriness.

arrival time of the k th presynaptic spike. g_{syn} represents the total conductance, integrated over the time course of the synaptic event, and thus has units nS msec. g_{syn} was taken from an exponential distribution with mean \bar{g}_{syn} ; values greater than $4\bar{g}_{\text{syn}}$ were then reset to this maximum value.⁸ For excitatory synapses, $V_{\text{ex}} = 0$ mV, and $\bar{g}_{\text{ex}} = 3.4$ nS msec. This yields EPSPs at rest of mean .49 mV and maximum 2 mV. For inhibitory synapses, $V_{\text{in}} = -70$ mV, and $\bar{g}_{\text{in}} = 22.8$ nS msec. This yields inhibitory postsynaptic potentials (IPSPs) that are twice as large as EPSPs at threshold.

The amount of inhibition was expressed as the ratio R of the mean inhibitory current to the mean excitatory current at threshold:

$$R = \frac{\lambda_{\text{in}} \bar{g}_{\text{in}} |V_{\text{in}} - V_{\text{thresh}}|}{\lambda_{\text{ex}} \bar{g}_{\text{ex}} |V_{\text{ex}} - V_{\text{thresh}}|} \quad (2.2)$$

Here λ expresses the mean rate of Poisson input. Note that $R = 1$ implies that when voltage is clamped at V_{thresh} , the total synaptic current has mean zero; $R < 1$ corresponds to a surplus of excitatory synaptic current at threshold, while $R > 1$ corresponds to a surplus of synaptic inhibition. The leak current adds hyperpolarizing current. Estimates for λ_{ex} and λ_{in} rely on counting arguments only weakly constrained by experimental data (Shadlen & Newsome, 1994). Thus, to examine how model behavior depends on λ_{ex} and λ_{in} , we fix R and then covary λ_{ex} and λ_{in} to yield varying output firing rates for that R . We have considered values of R ranging from 0 to 1.25; we will take $R = .75$ to be a reasonable guess for the ratio of inhibition to excitation in cortex.

Balanced inhibition models (Gerstein & Mandelbrot, 1964; Shadlen & Newsome, 1994) commonly assume equally likely positive and negative voltage steps, yielding a random walk in voltage. In a conductance-based model, this translates into a balance of inhibition and excitation sufficient to give a subthreshold mean current (so that there is not a steady drift up to near V_{thresh}). We will roughly equate balance inhibition with $R \geq 1$ (although smaller values are conceivable, since even for $R = 1$ the leak current maintains the mean voltage somewhat below threshold).⁹

3 Simulation Results

The results of a typical simulation ($R = .75$) are shown in Figure 1. Postsynaptic average firing rate was 98 Hz for 10 sec of simulated data. We measured variability by taking the CV of the ISI histogram, and found $CV = .6$, which falls in the physiological range of .5 to 1 reported in Softky and Koch (1993).

⁸ Thus the mean of the final distribution for g_{syn} is $(1 - e^{-4})\bar{g}_{\text{syn}}$.

⁹ The exact distance below threshold depends on the relative magnitudes of the leak and mean synaptic conductances. In the limit of high input rates, the leak is negligible, and $R = 1$ corresponds to a mean synaptic current just sufficient to elicit depolarization to threshold.

What expectations do we have for CV in these simple models? We expect CV to be bounded above by the CV of a Poisson process with dead time equal to the minimum recovery period. With mean ISI μ and dead time t_{dead} , $CV_{\text{max}} = (\mu - t_{\text{dead}})/\mu$. For the simulation in Figure 1, $t_{\text{dead}} = t_{\text{spike}}$ gives $CV_{\text{max}} = .83$, while taking t_{dead} equal to the shortest interval observed (2.75 msec) yields $CV_{\text{max}} = .73$.¹⁰ A rough lower bound can be obtained from the case of pure EPSP integration. In our high-gain model, it takes 16 average-sized EPSPs to reach threshold from reset (recall that EPSPs are reduced by three-fourths near threshold). Again accounting for dead time of $t_{\text{dead}} = t_{\text{spike}}$, a $1/\sqrt{N}$ argument yields $CV = .83\sqrt{16} = .2$. With variable-sized PSPs, this estimate should be adjusted upward by a factor of roughly $\sqrt{2}$ yielding $CV \approx .28$ (Softky & Koch, 1993; Stein, 1967). The reason that $1/\sqrt{N}$ arguments fail to estimate CV accurately will be discussed shortly.

We measured the dependence of CV on postsynaptic firing rate by varying input rates while keeping the inhibition-to-excitation ratio fixed at $R = .75$ (see Figure 2A). Physiologically reasonable levels of CV are obtained across firing rates. Also, CV decreases at higher firing rates, as observed experimentally (Softky & Koch, 1993, Fig. 3). To test the notion the a balance of excitation and inhibition is required to achieve high variability (Shadlen & Newsome, 1994; Bell et al., 1995), we varied the inhibition ratio R and observed ISI variability at input rates that yield postsynaptic firing rates between 95 and 105 Hz (see Figure 2B). To compare more closely with previous models that have used low gain, we also ran simulations with $V_{\text{reset}} = V_{\text{rest}}$. Balanced inhibition models are those with large R (e.g., $R = 1.25$),¹¹ while the low-gain model with excitation only ($R = 0$, marked "O") is similar to the simple EPSP integrator discussed in Softky and Koch (1993). The model with physiological (high) gain gives physiological CV over a broad range of R . In contrast, balanced inhibition ($R > 1$) is necessary to achieve $CV > .5$ in the low-gain model.

4 An Intuitive Picture

An intuitive grasp of spike variability in simple integrate-and-fire models can be obtained by roughly dividing the ISI into three regimes (see Figure 3A; see also Abeles, 1991, Chap. 4; Smith, 1992). In the initial refractory regime, the state of the neuron is dominated by the recovery from the previous spike. In this regime $1/\sqrt{N}$ arguments are valid (Smith, 1992), and spiking is regular. In the final, steady-state regime, the memory of the last spike has decayed and random synaptic variation causes the cell to fluctuate about

¹⁰ For a Poisson process with dead time, the shortest interval, the dead time, and the peak of the ISI distribution are the same.

¹¹ Shadlen and Newsome (1994) used $V_{\text{reset}} = V_{\text{rest}}$ and hence considered a low-gain balanced inhibition model.

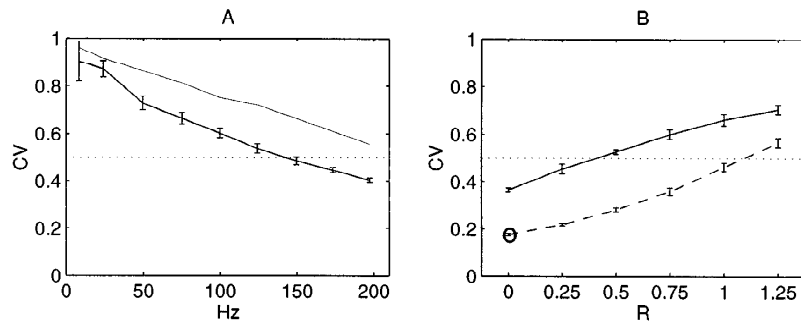


Figure 2: (A) CV versus output firing rate, for fixed inhibition ratio $R = 0.75$. Data shown are mean \pm standard deviation for 10 simulations (using different Poisson trains of inputs) of 10 sec duration. λ_{ex} ranged from 3396 Hz to 20,509 Hz, while λ_{in} correspondingly varied from 1274 Hz to 7691 Hz. The thin line shows CV for Poisson process with dead time equal to the shortest ISI observed. With increasing firing rate, the refractory period is a greater fraction of a typical ISI. Thus CV decreases with increasing rate. This effect is also seen in the biological data (Softky & Koch, 1993, Fig. 3). (B) CV versus inhibition ratio R for high gain (solid line; $V_{reset} = -60$ mV) and low gain (dashed line; $V_{reset} = V_{rest}$) models. $R = 1.25$ corresponds to example balanced inhibition models. Low gain with $R = 0$ corresponds to the EPSP integrator model (marked "O"). At a given level of R , values of λ_{ex} and λ_{in} were found for which the 95 percent confidence interval for the mean spike rate was within the range from 95 to 105 Hz (10 simulations of 10 sec each). Data shown are from 10 subsequent trials at these input rates. λ_{ex} ranged from 4448 Hz to 19,584 Hz for high gain and from 7500 Hz to 23,261 Hz for low gain; λ_{in} varied from 0 Hz to 12,240 Hz (high gain) and from 0 Hz to 14,538 Hz (low gain). The dotted line shows $CV = .5$.

some steady-state mean voltage (necessarily subthreshold). Thus, threshold crossings are equally likely to occur in any small interval and spike statistics are Poisson. In the intermediate regime, the mean voltage is still significantly rising, yet typical voltage fluctuations can be sufficient to cross threshold. Spike variability in this regime should be a mixture of $1/\sqrt{N}$ integration effects and Poisson random crossings. ISI variability depends on the relative amount of time spent in the regimes.

As shown in Figure 3B, integration in the EPSP integrator model is primarily in the refractory regime, and hence spiking is regular. In the low-gain balanced-inhibition model, large, transient changes in the balance of excitation and inhibition are large enough to dominate the cell's refractoriness

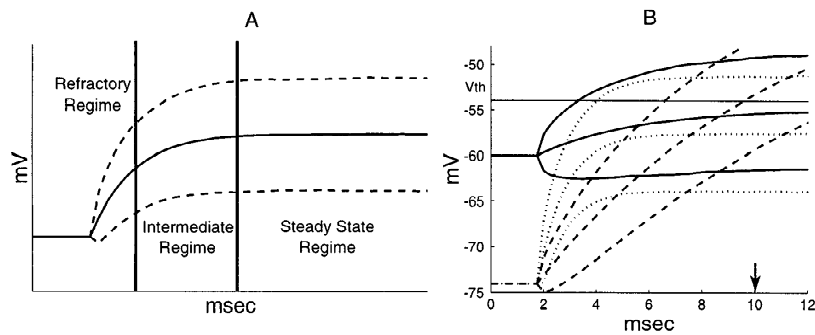


Figure 3: Mean \pm standard deviation of the distribution of voltages. (A) Schematic showing three regimes of behavior (see text). (B) Data obtained from repeated ($n = 10,000$) experiments starting the model (without spiking) from V_{reset} . Rates set to achieve firing rates of $100 (\pm 5)$ Hz. Solid lines are from the high-gain model ($V_{\text{reset}} = -60$ mV; $R = .75$; $\lambda_{\text{ex}} = 8885$ Hz; $\lambda_{\text{in}} = 3332$ Hz). Dashed lines are low-gain models ($V_{\text{reset}} = -74$ mV = V_{rest}). Dashed lines are from the EPSP integrator ($R = 0$; $\lambda_{\text{ex}} = 7500$ Hz; $\lambda_{\text{in}} = 0$ Hz). Dotted lines are from a low-gain, balanced-inhibition model ($R = 1.25$; $\lambda_{\text{ex}} = 23,261$ Hz; $\lambda_{\text{in}} = 14,538$ Hz). The arrow points to mean ISI.

rather quickly, and the cell spends most of its time in the intermediate and steady-state regimes. Note that this recovery is aided by a reduction of the membrane time constant due to the large synaptic conductance. The small reset of the high-gain model causes the cell to spend most of the time in the intermediate or steady-state regimes for virtually any input combinations that yield biologically reasonable firing rates.

Note that any mechanism that acts to reduce the importance of the transient, refractory regime contributes to variable spiking. In our model, V_{reset} is the dominant parameter determining the significance of the refractory regime. However, reducing the membrane time constant τ shortens transients and can emphasize steady-state behavior. Increasing the variability of the synaptic current results in a more rapid transition to the intermediate regime and hence will also increase spike variability. Thus balanced inhibition, which reduces τ and increases input variability, and high-gain mechanisms are independent effects that can contribute to variable spiking. It has been suggested (Bell et al., 1995) that spike variability depends on the cell's "hovering" near threshold, so that the integration of only a few inputs can cause a spike. While this is similar to our explanation of steady-state behavior, there is a significant difference. In the steady-state regime, threshold crossings result from random fluctuations in the input current,

so spiking is always Poisson, regardless of steady-state voltage level. Thus, the nearness to threshold in the steady-state regime affects spike rate but does not directly affect spike variability.

5 Discussion

We have shown that matching simple integrate-and-fire neurons to experimental data results in ISI distributions with physiological CV. In additional studies, we have found that high CV is also produced by more realistic integrate-and-fire models incorporating the finite time course of synaptic conductances, realistic combinations of fast and slow excitatory synapses (AMPA and NMDA), and spike rate adaptation. Lengthening the synaptic time course can result in input correlations longer than the shortest ISIs and lead to burstlike behavior that can actually increase CV; a realistic mixture of fast and slow synapses avoids such burstiness while achieving high CV.¹²

Does an understanding of the intermediate and steady-state regimes have implications for neural coding? In these regimes, both the mean synaptic current and the variance in this current contribute to neuronal spiking. A neuron operating in these regimes is certainly capable of rate coding—coding mean input rates with a mean output rate. When inputs are Poisson, the mean input rate of excitatory and inhibitory events determines both the mean and the variance of the total synaptic current and consequently the mean output rate. However, such a neuron is also capable, in principle, of responding to input fluctuations with high temporal resolution. The possible contributions of these different forms of coding will depend on signal-to-noise considerations—how reliably a given statistical attribute of the input can be transmitted and be distinguished from random input fluctuations—that will depend on the details of the statistics of the neuronal input. Thus, the fact of high CV alone does not serve to distinguish between “rate coding” and “coincidence detection” or “spike timing” models of neural encoding.

One difficulty with high-gain models is that they display low dynamic range; relatively small fluctuations in input current can lead to saturated outputs. In other studies (Troyer & Miller, 1995), we have found that spike rate adaptation helps to solve this problem by providing negative feedback that reduces gain on longer time scales, while preserving sensitivity to small input fluctuations on the time scale of typical interspike intervals. This fits well with the empirical observations that all excitatory cortical neurons show spike rate adaptation, while most inhibitory cortical neurons do not adapt but can sustain high rates of firing without saturating (McCormick et al., 1985).

¹² The burstlike behavior gives an unrealistically low CV², a measure of variability that compares only adjacent interspike intervals (Holt, Softky, Koch, & Douglas, 1996). The mix of fast and slow synapses gives a realistically high CV².

Our high-gain model results in ISI variability that falls in the lower half of the range .5 to 1 reported in Softky and Koch (1993). If one includes the refractory period, even a Poisson model cannot account for the upper reaches of these data. The most likely explanation is that cortical ISI variability results from a combination of mechanisms (including high gain) that have generally been explored in isolation. However, ISI variability alone is inadequate to distinguish the relative contributions of these mechanisms to cortical integration. Stronger constraints may be found from experiments designed to probe the biophysical basis of integration and spiking in cortical cells and from further statistical studies. The latter might examine, *in vivo*, the statistics of synaptically driven voltage and current fluctuations as well as spike train statistics beyond CV, and *in vitro*, the dependence of firing rate and CV on both mean and variance of white noise input current. One recent technique that may shed light on the contribution of cortical inhibition is the ability to block inhibitory input to a single cell pharmacologically (Nelson, Toth, Sheth, & Sur, 1994).

To understand cortical ISI variability, classical notions of neuronal integration must be modified, not by abandoning the integrate-and-fire neuron but by deepening our understanding of the dynamics of such model neurons. In particular, the common intuition of dynamics dominated by recovery, with $1/\sqrt{N}$ integration behavior, must be supplemented by an understanding of a regime in which spike behavior is Poisson. Such a regime has been well studied in voltage-based integrate-and-fire models using a variety of statistical approaches (Gerstein & Mandelbrot, 1964; Stein, 1967; Smith, 1992; Tuckwell, 1988, Chap. 9); in certain limits the regime can be described as an unbiased random walk of voltage with decay. The importance of such a random, steady-state regime for cortical processing has been discussed by several previous authors (Abeles, 1991; Shadlen & Newsome, 1994; Bell et al., 1995). Our contributions are to make specific links between refractoriness and neuronal gain and to demonstrate that an integrate-and-fire model fitted to known cortical physiology will operate in the intermediate and steady-state regimes for physiologically reasonable firing rates and a wide range of ratios of inhibition to excitation. In these regimes, variable spike statistics dominate, and hence the model produces physiological CV. Thus, in contrast to the intuition presented in Softky and Koch (1993), one should expect a high degree of ISI variability from cortical neurons. Of course, a full biophysical understanding of cortical integration may yet require abandonment of this simple view of cortical processing, but the fact of cortical ISI variability alone does not.

Acknowledgments

We thank Larry Abbott, Paul Bush, Mark Kvale, Anton Krukowski, Neal Hessler, and Svilen Tzonev for helpful comments on this article. This work

was supported by an NSF Mathematical Sciences Postdoctoral Research Fellowship (T.W.T.) and by a Whitaker Foundation Biomedical Engineering Research Grant, the Searles Scholars' Program, and the Lucille P. Markey Charitable Trust (K.D.M.).

References

- Abeles, M. (1982). Role of the cortical neuron: Integrator or coincidence detector? *Israel J. Med. Sci.*, *18*, 83–92.
- Abeles, M. (1991). *Corticonics: Neural circuits of the cerebral cortex*. Cambridge: Cambridge University Press.
- Alonso, J. M., Usrey, W. M. & Reid, R. C. (1995). Precisely correlated firing in cells of the lateral geniculate nucleus. *Nature*, *383*, 815–819.
- Bell, A. J., Mainen, Z. F., Tsodyks, M., & Sejnowski, T. J. (1995). *Balanced conductances may explain irregular cortical spiking* (Tech. Rep. No. INC-9502). San Diego, CA: Institute for Neural Computation, University of California at San Diego.
- Gerstein, G. L., & Mandelbrot, B. (1964). Random walk models for the spike activity of a single neuron. *Biophys. J.*, *4*, 41–68.
- Hansel, D., & Sompolinsky, H. (1996). Chaos and synchrony in a model of a hypercolumn in visual cortex. *J. Comput. Neurosci.*, *3*, 7–34.
- Holt, G. R., Softky, W. R., Koch, C., & Douglas, R. J. (1996). A comparison of discharge variability *in vitro* and *in vivo* in cat visual cortex neurons. *J. Neurophysiol.*, *75*(5), 1806–1814.
- McCormick, D. A., Connors, B. W., Lighthall, J. W., & Prince, D. A. (1985). Comparative electrophysiology of pyramidal and sparsely spiny stellate neurons of the neocortex. *J. Neurophysiol.*, *54*, 782–805.
- Nelson, S., Toth, L., Sheth, B., & Sur, M. (1994). Orientation selectivity of cortical neurons during intracellular blockage of inhibition. *Science*, *265*, 774–777.
- Shadlen, M. N., & Newsome, W. T. (1994). Noise, neural codes and cortical organization. *Curr. Opin. Neurobiol.*, *4*, 569–579.
- Smith, C. E. (1992). A heuristic approach to stochastic models of single neurons. In T. McKenna, J. Davis, & S. F. Zornetzer (Eds.), *Single Neuron Computation* (pp. 561–588). San Diego, CA: Academic Press.
- Softky, W., & Koch, C. (1993). The highly irregular firing of cortical-cells is inconsistent with temporal integration of random EPSPs. *J. Neurosci.*, *13*, 334–350.
- Stein, R. B. (1967). The information capacity of nerve cells using a frequency code. *Biophys. J.*, *7*, 797–826.
- Troyer, T. W., & Miller, K. D. (1995). A simple model of cortical excitatory cells linking NMDA-mediated currents, ISI variability, spike repolarization and slow AHPs. *Soc. Neuro. Abs.*, *21*, 1653.
- Tuckwell, H. C. (1988). *Introduction to theoretical neurobiology*. Cambridge: Cambridge University Press.
- Usher, M., Stemmler, M., Koch, C., & Olami, Z. (1994). Network amplification of local fluctuations causes high spike rate variability, fractal firing patterns and oscillatory local field potentials. *Neural Comp.*, *6*, 795–836.

Wilbur, W. J., & Rinzel, J. (1983). A theoretical basis for large coefficient of variation and bimodality in neuronal interspike interval distributions. *J. Theor. Biol.*, *105*, 345–368.

Received January 12, 1996; accepted July 29, 1996.